# Suppressing STAT3 activity protects the endothelial barrier from VEGF-mediated vascular permeability

Li Wang[1,#], Matteo Astone[1,#,£], Sk. Kayum Alam[1], Zhu Zhu[1], Wuhong Pei[2], David A. Frank[3], Shawn M. Burgess[2], Luke H. Hoeppner[1,4,*]

[1]The Hormel Institute, University of Minnesota, Austin, MN, USA.
[2]Translational and Functional Genomics Branch, National Human Genome Research Institute, National Institutes of Health, Bethesda, MD, USA.
[3]Department of Medical Oncology, Dana-Farber Cancer Institute, Boston, MA, USA.
[4]Masonic Cancer Center, University of Minnesota, Minneapolis, MN, USA.

[£]Current Address: Department of Biology, University of Padova, Padova, Italy.

[#]These first authors contributed equally.

*Corresponding Author:
Luke H. Hoeppner, Ph.D.
The Hormel Institute, University of Minnesota
801 16th Avenue NE
Austin, MN 55912
Phone: +1 (507) 437-9623
Email: hoepp005@umn.edu

**ABSTRACT:**

Vascular permeability can be triggered by inflammation or ischemia in the heart, brain, or lung, where it promotes edema, exacerbates disease progression, and impairs tissue recovery. Vascular endothelial growth factor (VEGF) is a potent inducer of vascular permeability, and VEGF plays an integral role in regulating vascular barrier function in physiological conditions and a variety of pathologies, such as cancer, ischemic stroke, cardiovascular disease, retinal conditions, and COVID-19-associated pulmonary edema and sepsis that often leads to acute lung injury, including acute respiratory distress syndrome. However, after initially stimulating permeability, VEGF subsequently mediates angiogenesis to repair damaged tissue following pathological injury. Consequently, understanding the molecular mechanisms of VEGF-induced vascular permeability will facilitate the development of promising therapies that achieve the delicate balance of inhibiting vascular permeability while preserving tissue repair mediated by VEGF signaling. Here, we demonstrate that VEGF signals through signal transducer and activator of transcription 3 (STAT3) to promote vascular permeability. Specifically, we show that STAT3 ablation reduces vascular permeability using endothelial cell-specific STAT3 knockout mice as well as VEGF-inducible zebrafish crossed with CRISPR-Cas9 generated genomic STAT3 knockout zebrafish. Importantly, STAT3 deficiency does not impair vascular development and function in these animals. Wildtype C57BL/6 mice treated with JAK2 inhibitor, AG490, exhibit decreased vascular permeability when measured in vivo by Miles permeability assay, confirming the role of JAK2 in VEGF-induced vascular permeability. Using human endothelial cells, we describe a novel mechanism of STAT3-dependent transcriptional regulation of intercellular adhesion molecule 1 (ICAM-1), an endothelial transmembrane protein involved in the regulation of vascular permeability. FDA-approved anti-microbial drug, pyrimethamine (PYR), has been identified as an inhibitor of STAT3 function at concentrations known to be safely achieved in humans. We report that PYR substantially reduces VEGF-induced vascular permeability in mice. We confirm that pharmacologically targeting STAT3 increases vascular barrier integrity in human endothelium using two additional STAT3 inhibitor compounds, including atovaquone, an FDA-approved anti-parasitic drug shown to inhibit STAT3-dependent transcription. Taken together, our findings suggest that the VEGF, VEGFR-2, JAK2, and STAT3 signaling cascade regulates vascular barrier integrity and compounds known to inhibit STAT3-dependent activity reduce VEGF-induced vascular permeability in vertebrate models.

## INTRODUCTION:

Proper physiological function relies on the vascular system to distribute oxygenating blood to all tissues, return deoxygenated blood to the lungs, and maintain tissue homeostasis, including functions such as hemostasis, lipid transport, and immune surveillance. In pathological conditions, vasculature is often adversely affected by the disease process, resulting in the development of vascular permeability[1]. Vascular endothelial growth factor (VEGF) is a central mediator of vascular permeability. In fact, VEGF was initially discovered as a tumor secreted factor that strongly promotes microvascular permeability named 'vascular permeability factor'[2] before its subsequent identification as VEGF[3], an endothelial mitogen essential for the development of blood vessels[4-6]. In cancer, VEGF-induced vascular permeability of plasma proteins creates a matrix amenable to vascular sprouting and tumor growth[2]. In addition to driving tumor angiogenesis, VEGF stimulates tumor cell extravasation, an important step in metastasis that enables cancer cells to enter the bloodstream and potentially invade other tissues[7]. Increased VEGF expression promotes hyperpermeability, edema, and tissue damage leading to the pathogenesis of cardiovascular disease, cerebrovascular conditions, retinal disorders, and acute lung injury. Acute lung injury, including acute respiratory distress syndrome, is among the most severe pathologies caused by coronavirus disease 2019 (COVID-19) and results in pulmonary edema caused by impaired vascular barrier function[8,9]. Autopsy reports of deceased COVID-19 patients frequently describe severe pulmonary mucus exudation, and acute lung injury is frequently a cause of death in severe cases of COVID-19[10,11]. A definitive treatment for acute lung injury does not exist. While therapeutically inhibiting vascular permeability reduces subsequent edema and tissue damage, VEGF-mediated angiogenesis is a key tissue repair mechanism[12,13]. Therefore, temporal VEGF modulation must be achieved when administering therapies to reduce edema and repair ischemic tissue damaged by pathogenesis, which underscores the importance of fully understanding the molecular and temporal regulation of vascular permeability in vivo.

Signal transducer and activator of transcription (STAT) proteins regulate a wide array of cellular functions, including proliferation, differentiation, inflammation, angiogenesis, and apoptosis[14]. Like most of its six other STAT protein family members, STAT3 was identified as part of a cytokine signaling cascade that potentiates the interleukin-6 (IL-6)-mediated hepatic acute phase response as a transcription factor[15,16]. In addition to its prominent role in IL-6 signal transduction, it is well established that VEGF signals through primarily VEGF receptor 2 (VEGFR-2) to stimulate STAT3 activation, dimerization, nuclear translocation, and DNA binding to regulate the transcription of genes involved in endothelial activation, vascular inflammation, and a variety of other biological processes[17-19]. Activation of STAT3 occurs through phosphorylation of tyrosine residue Y705[20]. Many STAT family members are phosphorylated by Janus kinases (JAKs), which are activated through trans-phosphorylation following ligand-mediated receptor multimerization. Mammalian JAK family members include JAK1, JAK2, JAK3 and TYK[21]. Reports across a variety of tumor and endothelial cell types have suggested members of the Janus kinase (JAK) family, Src, and the intrinsic kinase activity of VEGFR-2 as VEGF-induced activators of STAT3[22-26]. However, the precise mechanism through which VEGF/VEGFR-2 signaling promotes phosphorylation of STAT3 is poorly understood and likely tissue and cell type specific.

Here, we identify STAT3 as a central mediator of VEGF-induced vascular permeability. In our study, we exploit the strengths of three model systems, zebrafish, mice, and cultured human endothelial cells, to investigate the role of STAT3 in vascular permeability mediated by VEGF and VEGFR-2 signaling. Among other reasons, zebrafish (*Danio rerio*) have emerged as an invaluable vertebrate model of human pathophysiology due to their genetic similarity to *Homo sapiens* and the transparency of embryos that makes zebrafish amenable to *in vivo* fluorescent imaging[27]. We crossed previously described transgenic heat-inducible VEGF (iVEGF) zebrafish[28,29] to CRISPR/Cas9-generated STAT3 genomic knockout zebrafish[30] to evaluate the role of STAT3 in VEGF-induced vascular permeability *in vivo*. We establish a complementary VEGF-mediated vascular permeability model in endothelial cell-specific STAT3 knockout mice, demonstrate multiple pharmacological inhibitors of STAT3 reduce vascular permeability *in vivo*, and describe the molecular regulation of VEGF-induced vascular barrier integrity in human endothelial cells.

## MATERIALS AND METHODS:

### Cell culture

Human umbilical vein endothelial cells (HUVEC) and human pulmonary artery endothelial cells (HPAEC) were purchased from Lonza. Endothelial cells were seeded into plates that had been pretreated for 30 minutes with Collagen I (Corning, Catalog No. 354231). HUVEC were maintained in EBM Endothelial Cell Growth Basal

Medium (Catalog No. CC-3121, Lonza) supplemented with EGM Endothelial Cell Growth Medium SingleQuots (Catalog No. CC-4133, Lonza). HPAEC were cultured in EBM-2 Basal Medium (Catalog No. CC-3156, Lonza) supplemented with EGM SingleQuots (Catalog No. CC-4176, Lonza). HUVEC and HPAEC were certified prior to purchase, used exclusively at low passages, and authenticated by morphological inspection. For in vitro studies, HUVEC or HPAEC grown in culture to approximately 80% confluence were serum starved for 16 hours and subsequently stimulated with human recombinant VEGF-165 protein (25 ng/ml; R&D Systems; MNPHARM) for indicated durations. When applicable, cells were treated with inhibitors or control vehicle for various indicated periods of time following serum starvation and preceding VEGF-165 protein stimulation.

**Immunoblotting**

HUVEC were lysed in RIPA buffer (Millipore) containing protease inhibitor cocktail (Roche) and phosphatase inhibitor cocktail set V (Sigma). Proteins were separated via 4–20% gradient sodium dodecyl sulfate-polyacrylamide gel electrophoresis (Bio-Rad) and transferred to polyvinyl difluoride membranes (Millipore). Membranes were blocked with 5% bovine serum albumin (Sigma-Aldrich) and incubated with primary and secondary antibodies. Antibodies were purchased from Cell Signaling Technology (CST) to detect ZO-1 (Catalog No.13663; dilution 1:1000), phosphorylated VEGFR-2 (Tyr1175, Catalog No. 2478; dilution 1:1000), phosphorylated STAT3 (Tyr705, Catalog No. 9145; dilution 1:500), phosphorylated JAK2 (Tyr 1007/1008, Catalog No. 3771; dilution 1:500), phosphorylated JAK1 (Tyr 1034/1035, Catalog No. 3331S; dilution 1:500), phosphorylated TYK2 (Tyr1054/1055, Catalog No. 9321S; dilution 1:500), VEGFR-2 (Catalog No. 2479; dilution 1:1000), STAT3 (Catalog No. 12640; dilution 1:1000), JAK2 (Catalog No. 3230; dilution 1:500), JAK1 (Catalog No. 3332; dilution 1:500) and TYK2 (Catalog No. 14193; dilution 1:500). Additional antibodies were obtained from Santa Cruz Biotechnology to detect phosphorylated STAT3 (Tyr705, Catalog No. sc-8059; dilution 1:500), ICAM1 (Catalog No. sc-18853; dilution 1:500), and tubulin (Catalog No. sc-5286; dilution 1:500). The monoclonal antibody for detecting GST (Catalog No. MA4-004; dilution 1:1000) was bought from Thermo Fisher Scientific. Horseradish peroxidase-conjugated anti-rabbit (Catalog No. 7074; dilution 1:5000) and anti-mouse (Catalog No. 7076; dilution 1:5000) secondary antibodies (1 µg/µl) were purchased from Cell Signaling Technology. Antibody-reactive protein bands were detected by enzyme-linked chemiluminescence (Thermo Fisher Scientific) using an ImageQuant™ LAS 4000 instrument (GE Healthcare) and quantified using ImageJ software.

**Immunofluorescence**

HUVEC or HPAEC were seeded at 4 x $10^4$ cells per well onto EMD Millipore Millicell EZ Slides (PEZGS0416; Sigma Millipore), grown in complete medium for 48 hours, and subsequently serum starved for 16 hours. After receiving inhibitors and/or human recombinant VEGF-165 stimulation, cells were fixed in 4% paraformaldehyde (Boston Bioproducts), permeabilized in cold methanol (Fisher), and immunofluorescence staining was performed using antibodies against ZO-1 (CST, Catalog No.13663; dilution 1:200), p-STAT3 (Santa Cruz Biotechnology; Tyr705, Catalog No. sc-8059; dilution 1:50) or STAT3 (CST, Catalog No. 12640; dilution 1:100). The cells were then washed with PBS and incubated with CF™ 488A goat anti-rabbit secondary antibody (Sigma-Aldrich; Catalog No. SAB4600389; dilution 1:1000) or CF™ 594 goat anti-mouse secondary antibody (VWR; Catalog No. 20110; dilution 1:1000). Nuclei were stained using 4', 6-diamidino-2-phenylindole (DAPI; Cell Signaling; cat no.: 8961S). All images were captured on a Zeiss Apotome 2 microscope by using 20x, 0.8 NA Plan Apochromat objective magnifying 2X and processed using ImageJ software (Version 1.8.0_112; https://imagej.nih.gov/ij).

**Immunoprecipitation**

HUVEC were lysed in RIPA buffer (Millipore) supplemented with protease inhibitor cocktail (Roche) and phosphatase inhibitor cocktail set V (Sigma). After quantifying protein using the Quick Start Bradford protein assay (Bio-Rad), 500 µg protein lysate was loaded to the supplied spin column and immunoprecipitation was achieved following the manufacturer's protocol (Catch and Release Immunoprecipitation Kit; Catalog No.: 17-500; Millipore).

**Vascular permeability assay in mice**

$STAT3^{flox/flox}$ ($Stat3^{tm1Xyfu}$/J) and Tg(Tek-cre)1Ywa/J mice were purchased from The Jackson Laboratory. Genotyping primer pairs for genotyping the $Stat3^{tm1Xyfu}$/J mice are forward primer 5'-TTGACCTGTGCTCCTACAAAAA-3' and reverse primer 5'-CCCTAGATTAGGCCAGCACA-3'. The genotyping primer pairs for Tg(Tek-cre)1Ywa/J mice are forward primer 5'-CGCATAACCAGTGAAACAGCATTGC-3' and reverse primer 5'-CCCTGTGCTCAGACAGAAATGAGA-3'. Mice with endothelium-specific knockout of STAT3

were created by breeding transgenic mice STAT3$^{flox/flox}$ (Stat3$^{tm1Xyfu}$/J) with Tg(Tek-cre)1Ywa/J mice. C57BL/6 wildtype mice (Charles River, Catalog No. 027) were purchased and bred. Eight- to ten-week-old pathogen-free male and female mice housed in temperature-controlled room with alternating 12-hour light/dark cycles and fed a standard diet were used for vascular permeability experiments. To assess vascular permeability, Evans Blue (100 µl; 1% in PBS; VWR) was systemically injected in the lateral tail vein of mice. After 15 minutes, mice were anesthetized with ketamine (90-120 mg/kg)/xylazine (5-10 mg/kg) via IP injection, and 20 µl of PBS and VEGF solution (2.5 µg/ml in PBS; MNPHARM) were injected each in one anterior and one posterior footpad. After 30 minutes, the mice were euthanized and the footpads were excised. Evans Blue was extracted by incubation in formamide at 63°C overnight and quantified by spectroscopic detection at 620 nm using a Synergy Neo2 instument (BioTek). All mouse studies were performed in accordance with protocols approved by the University of Minnesota Institutional Animal Care and Use Committee.

**Assessment of vascular permeability in VEGF-inducible, STAT3 deficient zebrafish**

Transgenic VEGF-inducible zebrafish[28] were outcrossed to zebrafish heterozygous for STAT3 deficiency (STAT3$^{+/-}$) generated by CRISPR/Cas9 as previously described[30]. Subsequently, VEGF-inducible; STAT3$^{+/-}$ zebrafish were incrossed and the 1-cell stage embryos were microinjected with 1.5 nl of Cre mRNA (12.5 ng/µl). Zebrafish expressing the VEGF-inducible transgene were identified by the presence eGFP in their eyes using fluorescent imaging. At 2 days post-fertilization, 37°C heat shock of eGFP+ eyed zebrafish carrying the VEGF transgene was performed to confirm VEGF transgene activity via the absence of mCherry fluorescence. At 3 days post-fertilization, zebrafish were anesthetized and fluorescent microangiography was performed. A glass microneedle was inserted through the pericardium directly into the ventricle, and a mixture of 2000 kDa FITC-dextran and 70 kDa Texas Red-dextran (2 mg/ml in embryo water; Life Technologies, Inc.) was injected. Immediately prior to imaging, 37°C heat shock induction of the VEGF transgene was performed for 10 minutes. The visualization and real-time imaging were performed using the previously described SCORE methodology[31] on a Zeiss Apotome 2 microscope. Following imaging, each individual zebrafish was euthanized and genomic DNA was extracted using standard techniques for subsequent STAT3 genotyping using the following pair of primers: 5'-GGTCTTCCACAACCTGCTG-3' and 5'- TAGACGCTGCTCTTCCCAC-3'. Zebrafish were maintained in 28.5°C water in accordance with guidelines approved by the Institutional Animal Care and Use Committee at University of Minnesota. ImageJ software was used to quantitate the extent of Texas Red-dextran in the extravascular space. Mean gray value was measured after converting the image type to 8-bit gray, setting scale to pixels, inverting the image and identifying 4 areas of extravascular space in the middle of the zebrafish trunk region using drawing/selection tools to avoid intersegmental vessels evident by green fluorescent signal originating from FITC-dextran. The background gray value minus the average gray value of the four regions is used for statistical analysis.

**Compounds**

Pyrimethamine (PYR; 75 mg/kg; Sigma Aldrich) or control vehicle was delivered to mice by intraperitoneal injection daily for 15 days. PYR was dissolved in dimethyl sulfoxide (DMSO) to a concentration of 167 mg/ml and then diluted in PBS before injection into mice. Atovaquone (AQ; Sigma Aldrich) and C188-9 (Sigma Aldrich) were each dissolved in DMSO and used for in vitro studies at the indicated concentrations. C188-9 was bought from sigma (Catalog No. 573128). For in vivo studies, C188-9 was dissolved in DMSO at 208mg/ml and diluted in 5% dextrose in water (D5W) before injection. Mice received C188-9 (100 mg/kg) or vehicle (DMSO in D5W) by intraperitoneal injection daily for 1 week. For in vivo studies, Tyrphostin AG 490 (Sigma Aldrich) was dissolved in DMSO at the concentration of 250 mg/ml and diluted in PBS before injection**.** Mice received AG490 (1 mg per mouse) or vehicle (DMSO in PBS) by intraperitoneal injection daily for 1 week.

**Glutathione S-transferase (GST) pull-down assays**

The cDNA fragment encoding full-length human STAT3 was subcloned from pLEGFP-WT-STAT3[32] into the mammalian expression vector pEBG[33] using KpnI and NotI restriction enzyme sites and the following subcloning primer pairs: forward: 5'-GGGGTACCTCGAGCTCAAGCTTCAGGATGG-3' and reverse: 5'-ATAAGAATGCGGCCGCTCACTTGTAGTCCATGGGGGAGGTA-3'. pLEGFP-WT-STAT3 was a gift from Dr. George Stark (Addgene plasmid # 71450; http://n2t.net/addgene:71450; RRID:Addgene_71450)[32]. pEBG was generously shared by Dr. David Baltimore (Addgene plasmid # 22227; http://n2t.net/addgene:22227; RRID:Addgene_22227)[33]. Freestyle 293F cells (Thermo Fisher Scientific) grown in FreeStyle™ 293 Expression Medium (Thermo Fisher Scientific; 12338018) in an incubator at 37°C with 8% $CO_2$ were transfected with pEBG-STAT3 plasmid according to the instructions of the Freestyle 293 Expression System (Thermo Fisher Scientific) and then harvested by centrifugation at 1500 x g for 10 min. Cell pellets were

suspended in PBS containing protease inhibitor cocktail (Roche) and lysed on ice using 15 s pulses of sonication repeated 7 times with a Sonic Dismembrator, Model 100 (Fisher Scientific). Lysates in 1% Triton, 5 mM DTT were centrifuged at 12000g for 10 minutes at 4°C, and Glutathione Sepharose 4B (GE Healthcare) was used to bind the GST fusion proteins from the supernatant. GST protein-coated beads were incubated with pre-cleared HUVEC cell lysates at 4°C overnight. The bead-protein complexes were then washed 5 times with pre-chilled PBS, and the proteins were eluted using 10mM Glutathione elution buffer at room temperature. The proteins were boiled for 5 min in the Laemmli sample buffer and then analyzed by immunoblotting.

**Purification of human STAT3 protein**

STAT3 cDNA (human α isoform, residues 1-770) was subcloned from pLEGFP-WT-STAT3[32] into the RGS-6xHis-pcDNA3.1 plasmid[34], which was a gift from Dr. Adam Antebi (Addgene plasmid # 52534; http://n2t.net/addgene:52534; RRID: Addgene_52534)[34]. The 6xHis-STAT3α fragment was cloned into the pFastBac$^{TM}$Dial vector, generously provided by Dr. George Aslanidi at the University of Minnesota, The Hormel Institute. The plasmid was first transformed into *E. coli* DH10 MultiBac. Single colonies were inoculated into 2 ml antibiotic LB broth containing 50 µg/ml Kanamycin, 7 µg/ml Gentamycin, and 10 µg/ml Tetracycline and grown at 37°C overnight. After isolating recombinant Bacmid DNA, we transfected Sf9 insect cells, grew cells in Gibco™ Sf-900™ II SFM medium (Gibco, Catalog NO.10902088) in a 27°C incubator, harvested P0 baculovirus stock, and amplified P1 and P2 baculovirus in a 27°C, 90 rpm shaker. Sf9 cells were infected with P2 baculovirus (MOI=10) and cells were harvested by centrifugation at 1500 rpm for 10 minutes after incubation for 3 days. The pellet was resuspended in binding buffer [50 mM Tris-HCl (pH 8.0), 500 mM NaCl, 2 mM $MgCl_2$, 10% glycerol, 1mM Tris (2-Carboxyethyl) Phosphine (T-CEP), 10 mM Imidazole] supplemented with complete protease inhibitors (Roche) and then lysed by 7 cycles of sonication (Fisher Scientific; Sonic Dismembrator, Model 100) each consisting of constant pulse for 15s on ice. The lysate was cleared by centrifugation at 30,000 x g for 30 minutes at 4°C. The supernatant was bound to high performance HisTrap column (GE Healthcare) using binding buffer [Sodium phosphate 20 mM, NaCl 500 mM, Imidazole 20 mM and T-CEP 0.5 mM] and eluted with an imidazole gradient (0 to 500 mM). The protein was then concentrated and loaded onto a Superdex 200 size exclusion column equilibrated in 50 mM sodium phosphate, 150 mM NaCl and 0.5 mM T-CEP. Peak fractions were analyzed by SDS-PAGE.

**In vitro kinase assay**

Human JAK2 protein with active kinase activity (Signal Chem; J02-11G-05) and purified human STAT3 protein from Sf9 cells were subjected to an in vitro kinase assay using previously described methods[35]. Briefly, 10 µl JAK2 diluted in kinase dilution buffer III (Signal Chem; K23-09) to a final concentration of 0.1ug/ml was incubated with 3 µg purified STAT3 proteins as well as 5 µl ATP (New England Biolabs; N0440S) for 30 minutes at 30°C. The incubation was terminated by boiling the samples at $95^0$C for 5 minutes in 1X Laemmli sample buffer (Bio-Rad) supplemented with 10% β-mercaptoethanol (Bio-Rad). The samples were analyzed by immunoblotting using anti-phosphorylated STAT3 antibody (T705; Cell signaling Technology) to validate JAK2-mediated kinase activity upon STAT3 protein at Tyr705 position.

**Dual-luciferase reporter assay**

pGL3-ICAM1 luciferase reporter vector (pGL3-ICAM1-WT) was a generous gift from Dr. Jim Hu at the Hospital for Sick Children in Toronto, Ontario, Canada[36]. Site directed mutagenesis was performed to mutate the STAT3 binding site within the ICAM1 promoter from 5'-TTC-CxG-GAA-3' to 5'-AGC-CxC-CTG-'3. pGL3-ICAM1-mutant vector containing mutated STAT3 binding sites was generated by performing site-directed mutagenesis on pGL3-ICAM1-WT using QuikChange Lightning Site-Directed Mutagenesis Kit (Agilent) as previously described[37]. Constitutively active STAT3 plasmid EF.STAT3C.Ubc.GFP, with mutations A662C and N664C, was a gift from Dr. Linzhao Cheng (Addgene plasmid # 24983; http://n2t.net/addgene:24983; RRID: Addgene_24983)[38]. HUVEC were transfected with plasmids via electroporation using Neon Transfection system (Invitrogen) at a density of 1.5 x $10^6$ per sample and then seeded in collagen pre-coated 6-well plates. At 48 hours post transfection, cells were harvested following the instruction of Dual-Luciferase Reporter Assay System (Promega). Luminescence signals from firefly luciferase and renilla luciferase were measured in Synergy Neo 2 reader (BioTek).

**Statistical analysis**

Unpaired Student's t-test, a paired t-test or ANOVA was used to compare differences between groups as indicated and values of $P < 0.05$ were considered significant. Data are expressed as mean ± SEM and representative of at least three independent experiments.

## RESULTS:

### VEGF/VEGFR-2 induces STAT3 phosphorylation and nuclear localization

Given that we sought to investigate STAT3 as an important regulator of VEGF-induced vascular permeability, we first performed studies to confirm VEGF activates STAT3 in endothelial cells. We stimulated human umbilical vein endothelial cells (HUVEC) with VEGF, collected lysates, and performed immunoblotting. We observed activation of VEGFR-2 and STAT3 following 2 and 5 minutes of VEGF stimulation as evident by increased phosphorylation of VEGFR-2 Y1175 and STAT3 Y705 (**Figure 1A**), which coincides with prior reports[23]. VEGF stimulation promotes physical interaction of VEGFR-2 and STAT3, as evident by immunoprecipitation studies demonstrating an association of total VEGFR-2 and total STAT3 (**Figure 1B**) as well as VEGF-dependent interactions between the phosphorylated forms of VEGFR-2 and STAT3 (**Figure 1C**). To further study the interaction between VEGFR-2 and STAT3, we performed a GST pull-down experiment using GST-tagged STAT3 protein purified from 293F cells as a "bait" protein and growth factor (i.e. FBS) stimulated HUVEC lysate as a source of "prey" proteins. We observed a growth factor-dependent interaction between endothelial cell-derived VEGFR-2 and GST-tagged STAT3 proteins (**Figure 1D**). Immunofluorescence studies suggest that STAT3 translocates to the nucleus upon VEGF/VEGFR-2-mediated activation in HUVEC (**Figure 1E**). Quantification of nuclear STAT3 intensity showed a substantial increase upon VEGF treatment (**Figure 1F**). Collectively, our results suggest VEGF stimulates VEGFR-2 to induce STAT3 phosphorylation and nuclear localization in human endothelial cells.

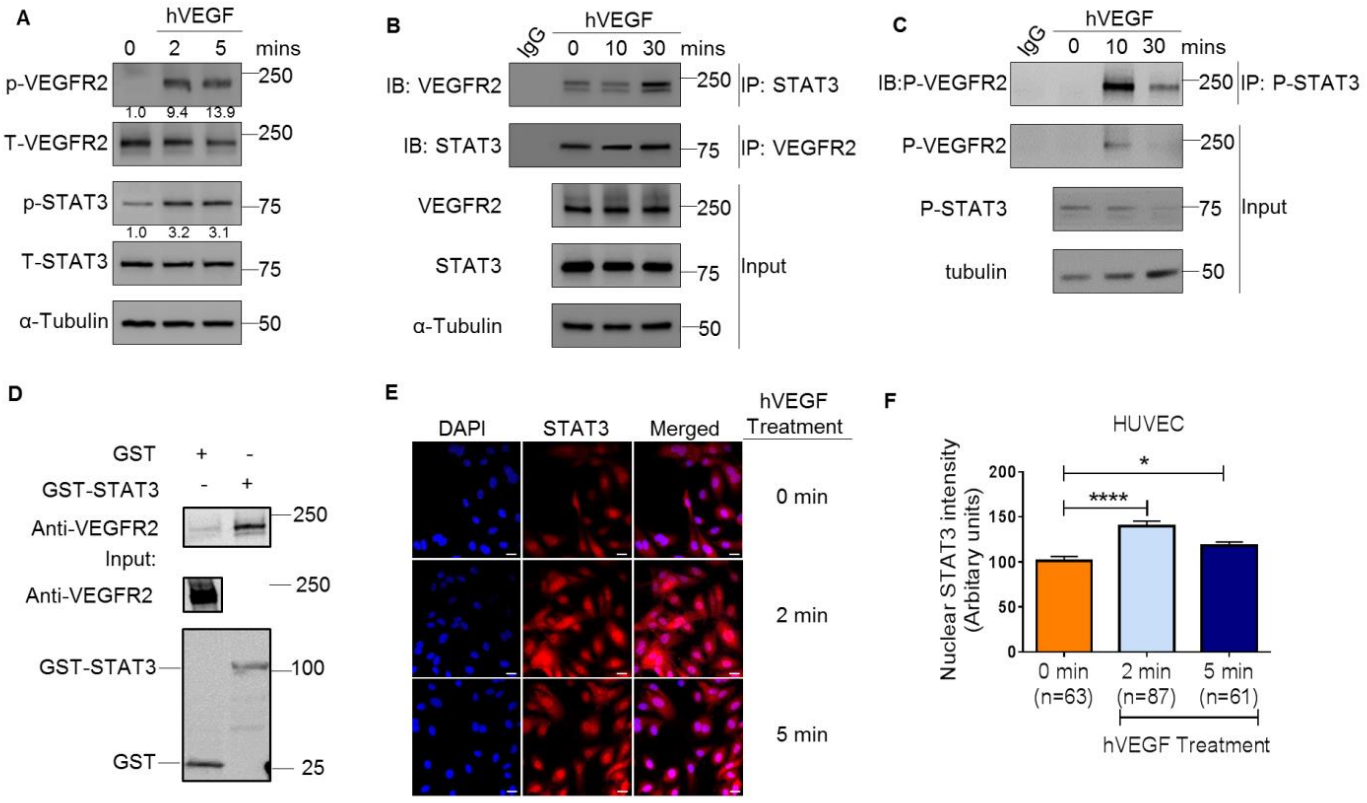


**Figure 1: VEGF/VEGFR-2 induces STAT3 phosphorylation and nuclear localization.** (A) Stimulation of HUVEC with 25ng/ml recombinant human VEGF-165 protein for 2 and 5 minutes induces p-VEGFR-2 (Y1175) and p-STAT3 (Y705) via immunoblotting. (B) VEGF (25 ng/ml) stimulation in HUVEC for 10 and 30 minutes promotes co-immunoprecipitation of STAT3 and VEGFR-2. (C) VEGF (25 ng/ml) stimulation in HUVEC for 10 and 30 minutes promotes co-immunoprecipitation of p-STAT3 (Y705) and p-VEGFR-2 (Y1175). (D) GST pull-down of VEGFR-2 with STAT3. Lysates of HUVEC stimulated with serum for 30 minutes were used as prey. GST fusion protein STAT3 expressed in 293F cells was used as bait. GST alone served as a negative control. Binding experiments were analyzed by SDS-PAGE and visualized by immunoblot. GST-STAT3 and GST were both detected using an anti-GST antibody. (E) VEGF stimulation for 2 minutes and 5 minutes promotes nuclear localization of STAT3. DAPI is blue. Scale bar, 20 μm. (F) Quantification of nuclear immunofluorescence staining intensity. Mean ±SEM, one-way ANOVA. *P<0.05, ****<0.00001. (A-E) Images are representative of multiple biological replicates.

## VEGF-induced vascular permeability is reduced in genomic STAT3 knockout zebrafish

To investigate the role of STAT3 in VEGF-induced vascular permeability *in vivo*, we utilized a heat shock inducible VEGF transgenic zebrafish (iVEGF) that we previously developed to identify regulators of VEGF-mediated vascular leakage[28,29]. Specifically, we generated STAT3 knockout zebrafish with an inducible VEGF transgene by crossing iVEGF zebrafish[28] to CRISPR/Cas9-generated STAT3 genomic knockout ($STAT3^{KO}$) zebrafish (**Figure 2A**). Importantly, we did not observe any vascular development defects in $STAT3^{KO}$ larval zebrafish, and the vascular system of $STAT3^{KO}$ zebrafish at 3 days post-fertilization (dpf) is indistinguishable from wildtype $STAT3^{+/+}$ siblings (**Figure 2B**). To assess vascular permeability, VEGF was heat-induced in $STAT3^{KO}$; iVEGF zebrafish following ventricular co-injection of 70 KDa Texas Red-dextran as a permeabilizing tracer and 2000 KDa FITC-dextran as a marker of the veins. Zebrafish were immediately live imaged using time-lapse structured illumination fluorescence microscopy to measure vascular permeability, evident by leakage of Texas Red-dextran into the extravascular space[28]. Using these techniques, our data showed decreased VEGF-induced vascular permeability in $STAT3^{KO}$ zebrafish relative to corresponding wildtype controls (**Figure 2C-D**), suggesting that VEGF signals through STAT3 to promote vascular permeability.

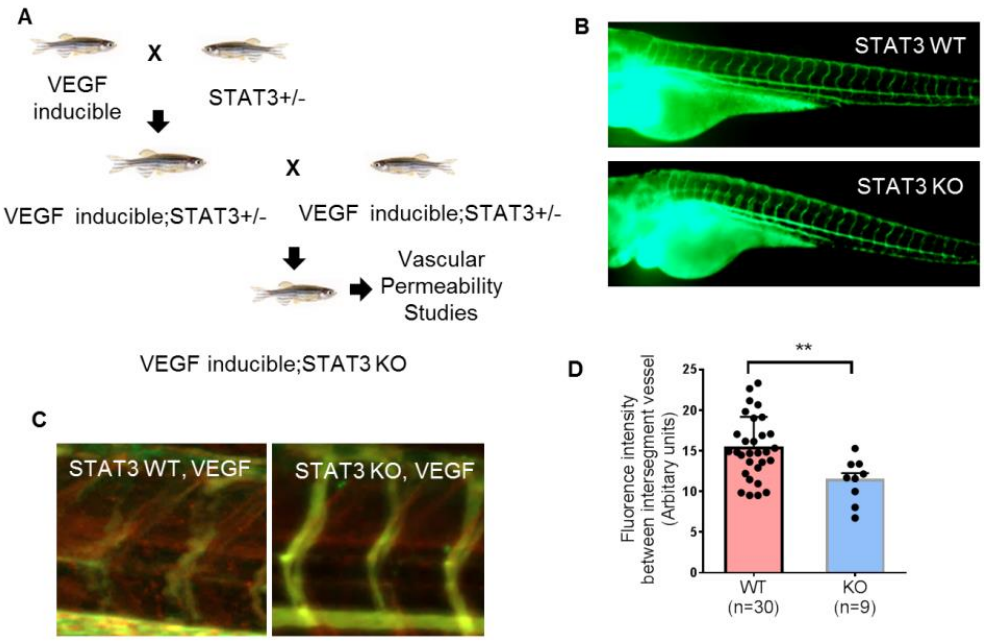


**Figure 2: VEGF-induced vascular permeability is reduced upon CRISPR-mediated knockout of STAT3 in zebrafish.** (A) VEGF-inducible zebrafish were crossed to STAT3+/- (heterozygous) zebrafish to generate VEGF-inducible; STAT3+/- double transgenic fish, which were intercrossed to generate VEGF-inducible; STAT3-/- (KO) zebrafish. (B) CRISPR/Cas9-generated STAT3 KO zebrafish display no overt vascular defects relative to WT. Vascular system visualized by microangiography with 2000 kDa FITC-dextran. (C) Microangiography using 70 kDa Texas Red-dextran permeabilizing tracer (red) and 2000 kDa FITC-dextran ISV marker (green) was performed on 3 day old VEGF-induced, $STAT3^{+/+}$ (n=30) and VEGF-induced, $STAT3^{-/-}$ (n=9) zebrafish. (D) The quantitative analysis of vascular permeability upon VEGF stimulation in wildtype ($STAT3^{+/+}$) and knockout ($STAT3^{-/-}$) zebrafish. **P<0.01, unpaired t-test (B, C) Representative images shown were obtained using a Zeiss Apotome 2 microscope with a Fluar 5x, 0.25 NA lens at RT. ISV: inter-segmental vessel.

## Endothelial-specific STAT3 knockout mice exhibit decreased VEGF-induced vascular permeability

To corroborate findings from the zebrafish vascular permeability model in a mammalian system, we have standardized a mouse footpad permeability assay in endothelial cell specific-STAT3 deficient mice ($STAT3^{ECKO}$). Given that germline STAT3 deficiency leads to embryonic lethality in mice[39], we generated endothelial cell specific-STAT3 deficient mice ($STAT3^{ECKO}$) by crossing Tie2-Cre mice[40] to STAT3 floxed mice[41]. To assess VEGF-induced vascular permeability by Miles assay, anesthetized $STAT3^{ECKO}$ or corresponding control mice were injected intravenously with Evans blue dye, and subcutaneously injected with recombinant VEGF protein (2.5 µg/ml in PBS; left footpads) or vehicle (right footpads). After 30 minutes, footpads were excised from euthanized mice, extravasated dye was extracted via formamide, and measured by spectrometry to quantify VEGF-induced vascular permeability. We observed significantly decreased extravasation of Evans blue dye in $STAT3^{ECKO}$ mice relative to wildtype controls, suggesting STAT3 is an important transducer of VEGF-induced vascular permeability (**Figure 3**).

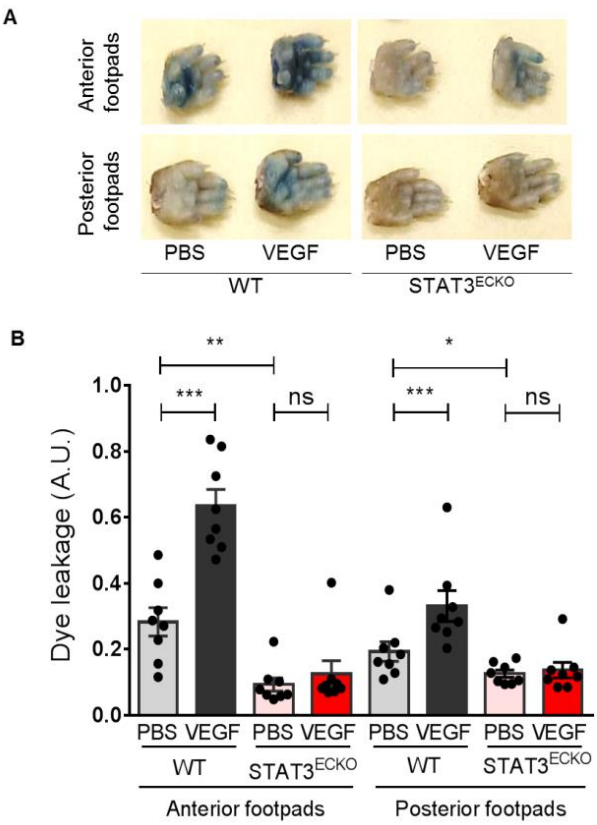


**Figure 3: Endothelial cell-specific STAT3 knockout mice exhibit decreased VEGF-induced permeability.** (A) Images of footpads from WT and STAT3$^{ECKO}$ (endothelial cell-specific STAT3 KO) mice following tail vein injection with 1% Evans blue and human recombinant VEGF-165 protein (2.5 µg/ml) or PBS vehicle being injected into the root of the footpad. (B) Quantitation of Evans blue leakage in Tie2-Cre negative; STAT3$^{flox/flox}$ (WT) and Tie2-Cre positive; STAT3$^{flox/flox}$ (STAT3$^{ECKO}$) mice. n=8 mice per group. Each mouse was injected with PBS on right anterior and posterior footpads and VEGF on left anterior and posterior footpads. Multiple biological replicates were performed and depicted findings are representative. *P<0.05, **P<0.01, ***P<0.001, one-way ANOVA followed by Dunnett's test.

**Pharmacological inhibition of STAT3 stabilizes endothelial barrier integrity following VEGF stimulation**

Given that genetic ablation of STAT3 reduces vascular permeability in zebrafish and mice, we sought to test the effects of pharmacological STAT3 inhibition on endothelial barrier integrity. Pyrimethamine (PYR)[42] and Atovaquone (AQ; Mepron®)[43] are FDA-approved antimicrobial agents that were recently discovered as new STAT3 inhibitors. AQ rapidly and specifically downregulates cell-surface expression of glycoprotein 130, which is required for STAT3 activation in multiple contexts. PYR was identified as a STAT3 inhibitor through a chemical biology approach. These compounds have been shown to be safe in humans because they inhibit STAT3 at concentrations routinely achieved in human plasma[42-44]. To our knowledge, PYR and AQ have yet to be specifically assessed in endothelium as prior studies have primarily evaluated their STAT3 inhibitory effects on tumor cells of epithelial origin. Therefore, we first treated HUVEC with various concentrations of PYR or AQ for different durations of time to determine the optimal conditions, while not exceeding the concentrations typically achieved in human plasma **(Supplemental Figure 1)**. In serum-starved HUVEC treated with 10 µM PYR for 1 hour or 30 µM AQ for 4 hours followed by VEGF stimulation, we observed decreased phosphorylation of STAT3 at Y705 **(Figure 4A-B)**. We confirmed activation of VEGF signaling by assessing the phosphorylation status and total protein levels of VEGFR-2 and JAK family members **(Figure 4A-B)**. Given that VEGFR-2, JAK1, JAK2, and TYK2 are upstream of STAT3, PYR- and AQ-mediated STAT3 inhibition does not affect activation of these proteins. Taken together, these immunoblotting results suggest PYR and AQ inhibit VEGF-induced STAT3 activation in human endothelial cells.

As vascular barrier stability is in large part regulated by intercellular junctions[45], we examined whether STAT3 inhibition affects junctional organization in human endothelial cells. We confirm by immunofluorescence that VEGF induces zonula occludens 1 (ZO-1) disorganization, indicative of tight junction instability **(Figure 4C)**. VEGF stimulation of HUVEC results in STAT3 activation as evident by increased phosphorylation of STAT3 Y705 **(Figure 4C-D)**. STAT3 pharmacological inhibition via PYR or AQ restores ZO-1 organization, suggesting that VEGF may mediate vascular permeability through STAT3-regulated control of ZO-1 (**Fig. 4C-D**). Correspondingly, we demonstrate that C188-9, a high-affinity inhibitor of STAT3 that targets its phosphotyrosyl peptide binding site within the SRC homology 2 (SH2) domain[46], prevents VEGF-mediated ZO-1 disorganization in HUVEC and HPAEC **(Supplemental Figure 2A-D)**.

Given that genetic ablation of STAT3 in mice and zebrafish reduces VEGF-mediated vascular permeability, we next sought to assess the effects of pharmacological STAT3 inhibition on endothelial barrier integrity in mice. To evaluate permeability upon STAT3 inhibition in vivo, we treated wildtype C57BL/6 mice with 75 mg/kg PYR daily for 15 consecutive days, 100 mg/kg C188-9 daily for 7 consecutive days, or each corresponding vehicle control via intraperitoneal injection, followed by Miles assay, which was performed as described for similar experiments. We observed decreased VEGF-induced extravasation of dye in mice treated with STAT3 inhibitor relative to controls, suggesting that pharmacological inhibition of STAT3 reduces vascular permeability in mice **(Figure 4E-F, Supplemental Figure 2E)**.

**JAK2 activates STAT3 to promote VEGF/VEGFR-2-induced vascular permeability**

Phosphorylation of STAT3 at Y705 causes its dimerization, nuclear translocation, and DNA binding to control transcription of genes, including regulators of vascular permeability. The kinase(s) that phosphorylates STAT3 Y705 in endothelial cells has not been well-identified. VEGF signals through VEGFR-2, which possesses intrinsic kinase activity through which it may activate STAT3 directly or through another kinase, such as JAK1, JAK2, JAK3, TYK2, or SRC[22-24,26]. Collective prior work supports the notion that the identity of the VEGF signaling-dependent kinase that activates STAT3 is cell type specific[22-26], but precise details remain poorly understood. Here, our findings suggest that JAK2 phosphorylates STAT3 in HUVEC and show JAK2 is required for VEGF/VEGFR-2-mediated vascular permeability in vivo. Specifically, we first tested whether JAK2 physically interacts with STAT3. Indeed, in GST pulldown assays purified GST-STAT3 fusion protein associates with each of VEGFR-2 and JAK2 present in lysates derived from stimulated HUVEC **(Figure 5A)**. To determine whether JAK2 directly phosphorylates STAT3, we performed an in vitro kinase assay using kinase active JAK2 protein with STAT3 protein we purified from Sf9 insect cells and found that JAK2 phosphorylates STAT3 at Y705 **(Figure 5B)**. Based on these findings, we hypothesized that VEGF/VEGFR-2 mediates activation of STAT3 through JAK2, which suggests JAK2 is required for VEGF-induced vascular permeability. To test the role of JAK2 in the regulation of vascular barrier integrity, we administered a JAK2 inhibitor, AG490, to C57BL/6 mice daily for seven consecutive days and assessed VEGF-induced vascular permeability by Miles assay. Specifically, anesthetized C57BL/6 mice were injected intravenously with Evans blue dye and subcutaneously injected with recombinant VEGF protein or vehicle control in the footpads. Pharmacological inhibition of JAK2 substantially reduced VEGF-mediated vascular permeability in mice **(Figure 5C-D)**, suggesting vascular permeability induced by VEGF/VEGFR-2 requires JAK2. Based on our collective findings, JAK2 activates STAT3 via Y705 phosphorylation to promote VEGF/VEGFR-2-induced vascular permeability.

**STAT3 transcriptionally activates ICAM1, a cell adhesion molecule that promotes vascular permeability**

We next sought to investigate molecular mechanisms through which STAT3 transcriptionally regulates VEGF-induced vascular permeability. To that end, we identified a novel STAT3 binding site within the promoter region of ICAM-1 **(Figure 6A)**, a cell adhesion molecule known to promote vascular permeability. Using luciferase-based reporter assays, we demonstrate increased ICAM-1 promoter activity upon co-transfection with increasing amounts of constitutively active STAT3 cDNA plasmid (**Figure 6B**). Mutation of the STAT3 binding site within the ICAM-1 promoter region prevents activation of the ICAM-1 promoter by constitutively active STAT3 (**Figure 6C**). Finally, we confirmed that ICAM-1 protein is upregulated following VEGF-mediated activation of STAT3 in human endothelial cells **(Figure 6D)**. Taken together, our findings suggest VEGF-induced STAT3 transcriptionally regulates ICAM-1 in human endothelium.

**DISCUSSION:**

Despite the prominent role of VEGF-induced vascular permeability in pathogenesis, a greater collective molecular understanding of its regulatory mechanisms is necessary to therapeutically improve vascular barrier integrity to prevent subsequent edema and tissue damage in vascular diseases like myocardial infarction, ischemic stroke, and acute lung injury. These research efforts have been hindered by limitations and inconsistencies in current accessible models. Endothelial cell culture models often fail to uniformly replicate in vivo models of hyperpermeability[28,47,48]. Molecular regulation of vascular barrier integrity can vary greatly based on various pathophysiological contexts and differences in cell types, tissues, anatomical locations, and species[28,49]. To overcome these obstacles, we took advantage of a transgenic VEGF-inducible zebrafish model that is amenable to genetic manipulation and reproducible live imaging of vascular permeability in optically clear zebrafish embryos using fluorescently labeled tracers[28,29]. Additionally, the widespread recent emergence of CRISPR/Cas9 genome editing techniques have enhanced the study genetic regulators of endothelial barrier function in genetically engineered zebrafish mutants.

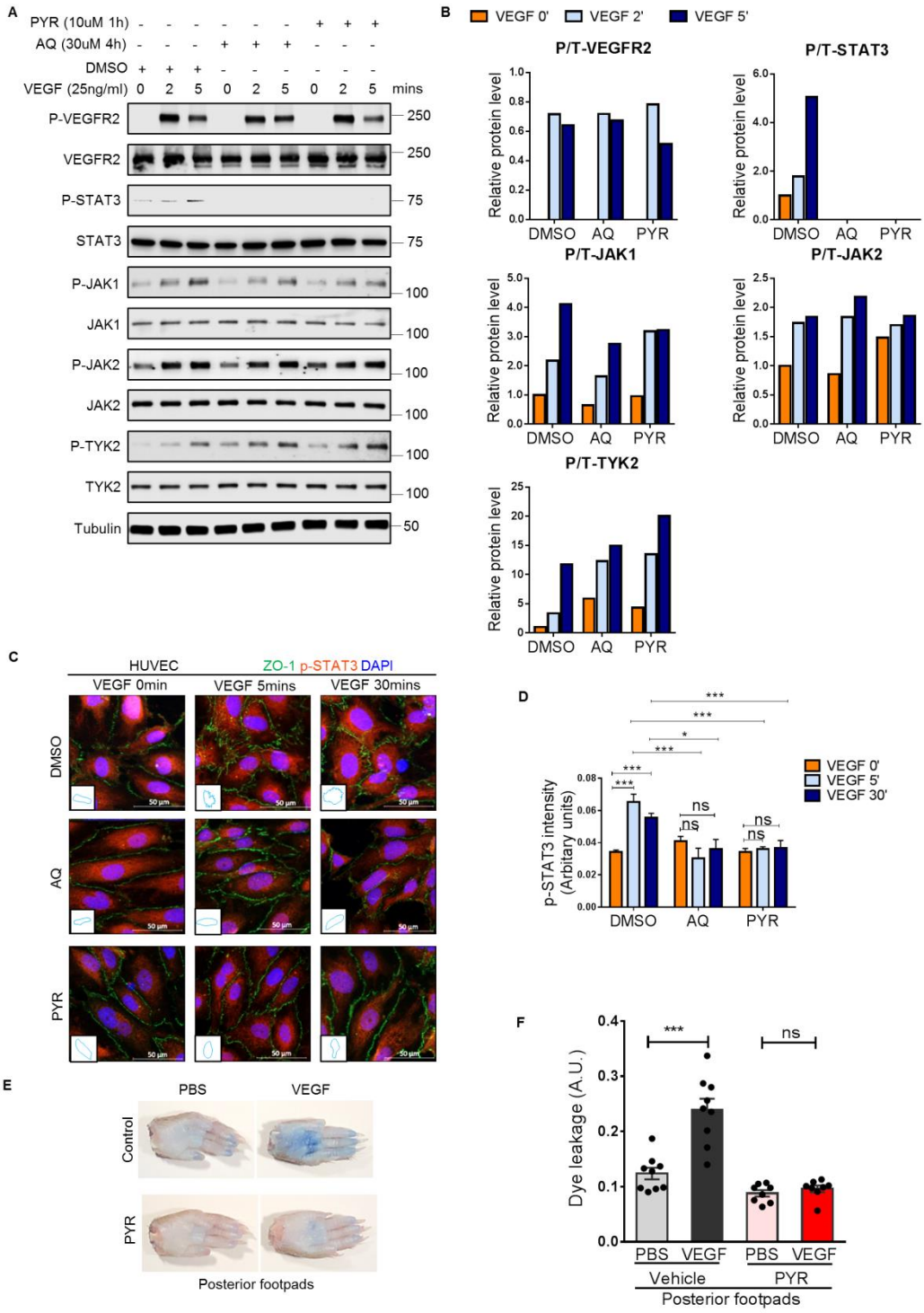


**Figure 4: Pharmacological inhibition of STAT3 stabilizes endothelial barrier integrity following VEGF stimulation in HUVEC and mice.** (A) Serum-starved HUVEC were pretreated with DMSO (vehicle control) for 1 hour, 30 μM AQ for 4 hours, or 10 μM PYR for 1 hour prior to human VEGF-165 recombinant protein (25 ng/ml) stimulation for 0, 2 or 5 minutes. Lysates were immunoblotted. (B) Densitometry quantification of phosphorylated protein relative to total protein. (C) VEGF stimulation of HUVEC promotes ZO-1 (green) disorganization at endothelial cell junctions (top: DMSO vehicle control pretreatment for 1 hour prior to VEGF stimulation). ZO-1 organization is maintained upon pretreatment with 30 μM AQ for 4 hours (middle) or 10 μM PYR for 1 hour (bottom) prior to VEGF stimulation. VEGF-induced phosphorylation of STAT3 at Y705 (p-STAT3; red) was reduced upon AQ or PYR pretreatment. Nuclei: DAPI (blue). Insets: ZO-1 staining trace of 1 representative cell/field. (D) Quantification of p-STAT3 (red). *P<0.05, ***P<0.001, one-way ANOVA. (E) Images of footpads from mice treated with vehicle or PYR following tail vein injection with 1% Evans blue and footpad injection of VEGF (2.5ug/ml) or PBS vehicle. (F) Quantitation of Evans blue leakage in C57BL/6 wildtype mice treated with vehicle or PYR. n=8 mice per group. Each mouse was injected with PBS on right anterior and posterior footpads and VEGF on left anterior and posterior footpads. Multiple biological replicates were performed and depicted findings are representative. ***P<0.001, paired t-test.

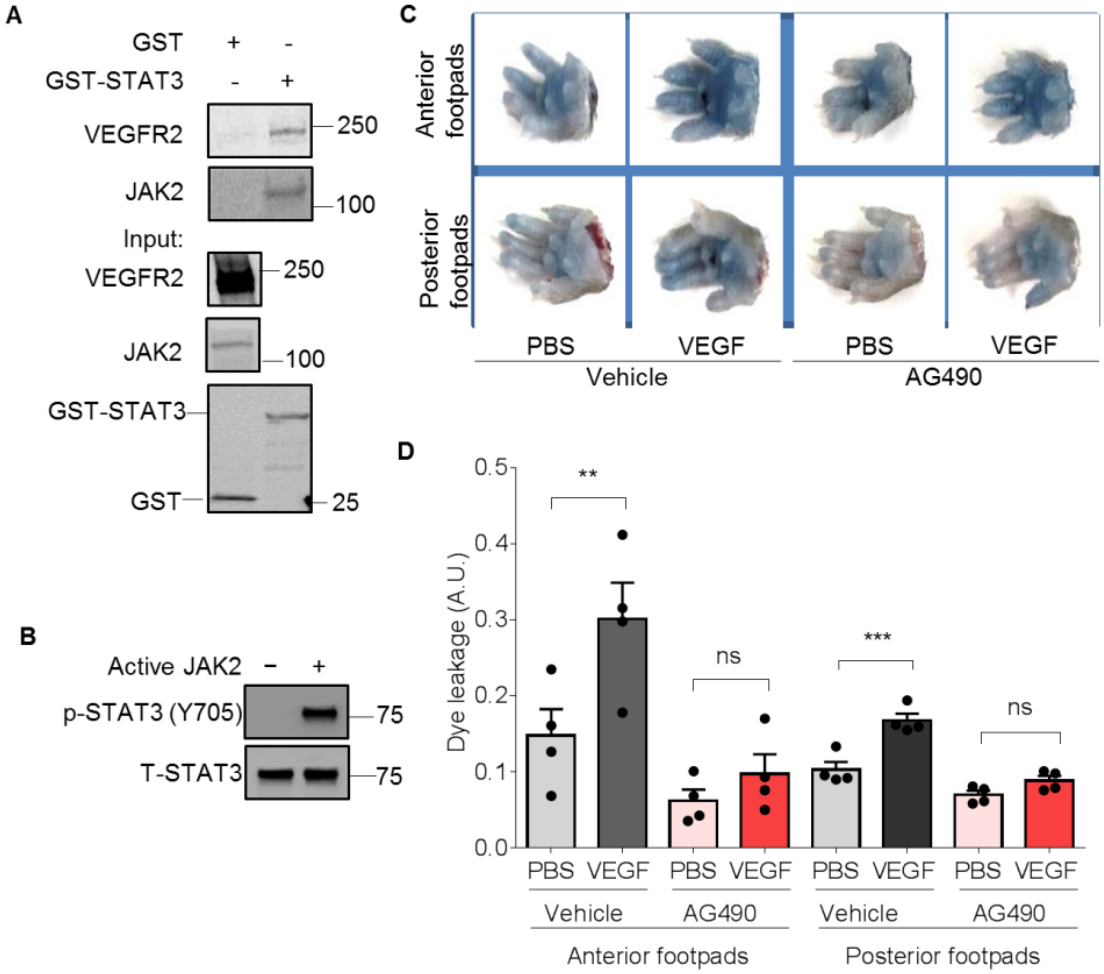


**Figure 5: JAK2 phosphorylates STAT3 to transduce VEGF/VEGFR-2 signaling and promote vascular permeability.** (A) To perform a STAT3 GST pull-down of VEGFR-2 and JAK2, lysates of HUVEC stimulated with serum for 30 minutes were used as prey. GST fusion protein STAT3 expressed in 293F cells was used as bait. GST alone served as a negative control. Binding experiments were analyzed by SDS-PAGE and visualized by immunoblotting. GST-STAT3 and GST were each detected using an anti-GST antibody. (C) JAK2 phosphorylates STAT3 in vitro. In vitro kinase assay was performed using purified human STAT3 protein and kinase active JAK2 protein. (D) Images of footpads from C57BL/6 wildtype mice treated with vehicle or JAK2 inhibitor AG490. Following tail vein injection with 1% Evans blue, human VEGF-165 protein (2.5 ug/ml) or PBS vehicle were injected into the root of the footpad. After 30 minutes, the mice were euthanized and the footpads were excised. (E) Quantitation of Evans blue leakage in C57BL mice treated with vehicle or AG490. N=5 mice per group. Each mouse was injected with PBS on right anterior and posterior footpads and VEGF on left anterior and posterior footpads. **P<0.01, ***P<0.001, paired t-test.

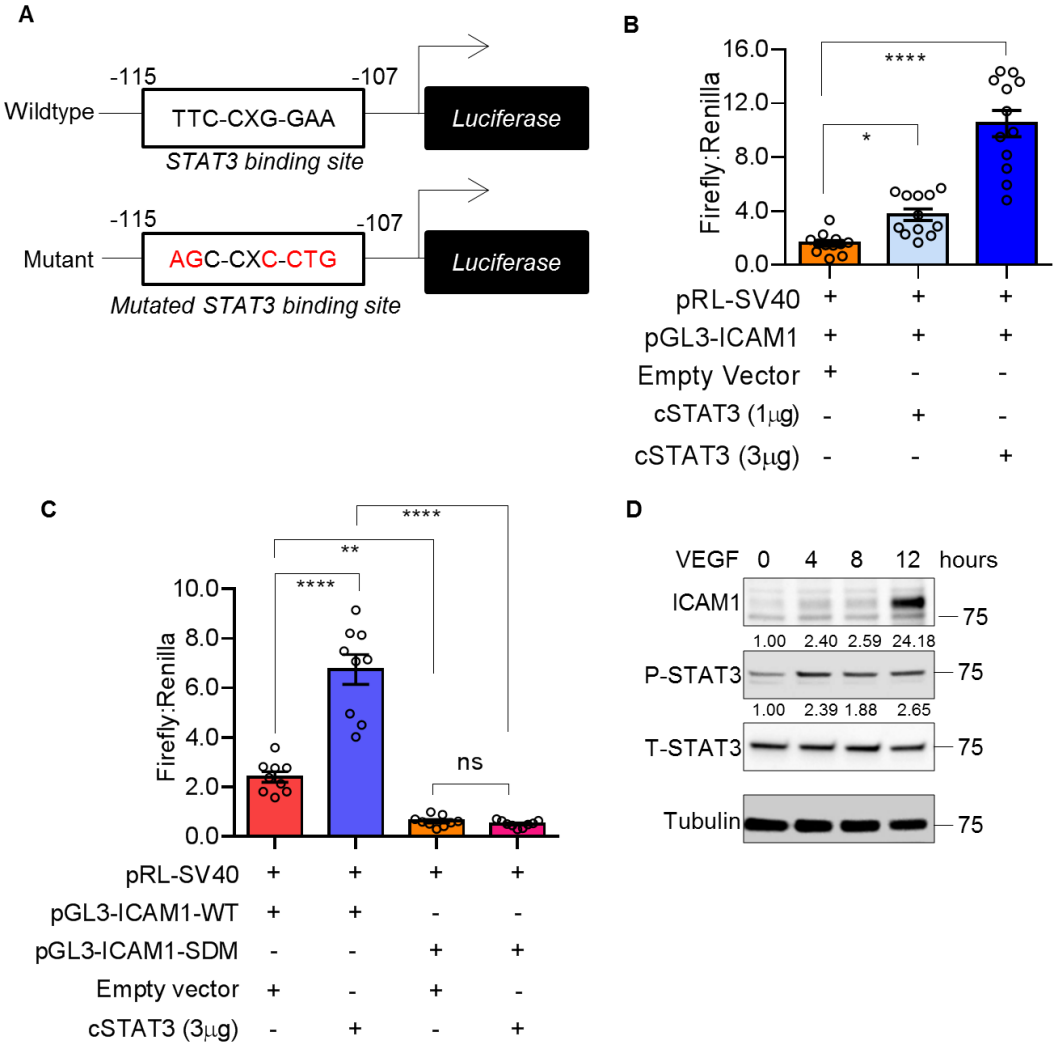


**Figure 6: STAT3 transcriptionally activates ICAM1, a cell adhesion molecule that promotes vascular permeability.** (A) The pGL3-ICAM1-WT plasmid (top) containing the human ICAM1 promoter with a STAT3 binding site located at -115 to -107bp. The pGL3-ICAM1-SDM plasmid (bottom) with mutation in the STAT3 binding site as indicated. (B) HUVEC were transiently transfected via electroporation with pGL3-ICAM1-WT (Firefly), pRL-SV40 (Renilla) plasmids and different amounts of constitutively active STAT3 plasmid (1 µg and 3 µg) using Neon transfection system. Firefly and Renilla luminescence was measured and plotted as ratio. Mean ±SEM, two-tailed unpaired t-test. n=12 technical replicates. *P<0.05, ****P<0.0001. (C) Dual-luciferase assays were performed in HUVEC that were transfected with pGL3-ICAM1-WT or pGL3-ICAM1-SDM and empty vector or constitutively active STAT3. Firefly and Renilla luminescence was measured and plotted as a ratio. Mean ±SEM, two-tailed unpaired t-test. n=9 technical replicates. **P<0.01, ****P<0.0001. (D) Human VEGF-165 protein (25 ng/ml) stimulated HUVEC lysates were immunoblotted for ICAM1, p-STAT3 (Y705), and total STAT3. (B-D) Depicted data is representative of multiple biological replicates. SDM: Site-directed mutagenesis.

In this study, we show the integral role of STAT3 in the molecular regulation of vascular permeability using VEGF-inducible zebrafish crossed to CRISPR/Cas9-generated STAT3 mutants. Genomic ablation of STAT3 substantially reduces VEGF-mediated extravasation of fluorescent dextran from intersegmental vessels within the trunk region of larval zebrafish. Correspondingly, genetic knockout of STAT3 in the endothelium of mice increases vascular barrier integrity. Pharmacological inhibition of STAT3 using PYR, AQ, and C188-9 reduces VEGF-mediated vascular permeability in wildtype mice and prevents tight junction disorganization typically caused by VEGF stimulation of cultured human endothelial cells.

In response to a variety of cytokines, growth factors, and hormones, STAT proteins are activated via phosphorylation, dimerize, translocate to the nucleus, and bind to specific target gene promoters to regulate cellular processes, such as proliferation, differentiation, migration, and survival[21]. Reports have demonstrated VEGF rapidly induces STAT3 tyrosine phosphorylation and nuclear translocation in microvascular endothelial cells[22-24,50]. A positive feedback loop exists as VEGF-induced STAT3 has been shown to be a direct transcriptional activator of the VEGF promoter[49,51]. Functionally, phosphorylation of STAT3 by VEGF/VEGFR-2 signaling is required for microvascular endothelial cell migration[24]. Correspondingly, VEGF-induced STAT3 phosphorylation has been shown to increase human cancer cell migration and invasion[52]. VEGF-mediated STAT3 activation also has been shown to promote human umbilical vein endothelial cell (HUVEC) survival through induction of anti-apoptosis molecule Bcl-2[23]. The findings presented here suggest that VEGF/VEGFR-2 signaling results in JAK2-mediated activation of STAT3, which enables STAT3 to translocate to the nucleus and transcriptionally regulate genes involved in vascular barrier integrity, including ICAM-1.

While genomic STAT3 deficiency in mice results in embryonic lethality, the endothelium tissue-specific STAT3 knockout mice we report here are healthy and fertile, which coincides with previous findings. Correspondingly, we observe normal vascular development in CRISPR/Cas9-generated zebrafish with homozygous genomic STAT3 deficiency using fluorescent microangiography for visualization. In vitro studies suggest that a dominant-negative form of STAT3 suppresses human dermal microvascular endothelial cell tube formation on Matrigel and collagen[24]. However, endothelial cells isolated from endothelium-specific STAT3 knockout mice and cultured ex vivo initiate normal tube formation[53]. While endothelial cell-specific STAT3 knockout mice undergo physiologically normal developmental angiogenesis, these mice exhibit defects in tissue repair and decreased recovery from vascular injuries, including myocardial infarction, cerebral ischemia, and ischemia-reperfusion injuries[47,48,54]. These observations highlight the need to understand the temporal dynamics through which STAT3 regulates pathological vascular permeability and edema as well as restorative angiogenesis to repair damaged tissue.

The functional role of STAT3 in VEGF-induced permeability has not been directly investigated. Prior studies suggest other permeability inducers, such as IL-6, IgG, IgE, histamine, lipopolysaccharides, and eotaxin, mediate vascular permeability through STAT3 signaling[25,55-61]. For example, an *in vitro* study using human endothelial cells recently demonstrated that IL-6 promotes sustained loss of endothelial barrier function via STAT3 signaling[55], and IL-6-induced STAT3 activation has been shown to induce vascular permeability in ovarian endothelial cells[60]. Furthermore, IL-6-induced retinal endothelial permeability was found to be dependent upon STAT3 activation in mouse retina by measuring leakage of Evans blue dye following IL-6 stimulation in the presence and absence of an inhibitor of STAT3 phosphorylation[61]. Dominant negative STAT3 has been shown to reduce IL-6-induced vascular permeability associated with malignant pleural effusion in lung adenocarcinoma[25] as well as decrease IgG-mediated vascular permeability in a mouse acute lung injury model[59]. Patients and mice harboring STAT3 mutations, which cause autosomal dominant hyper-IgE syndrome (AD-HIES), have been shown to be partially protected from anaphylaxis. Based on this finding, Hox and colleagues have shown that HUVEC derived from patients with AD-HIES or treated with a STAT3 inhibitor exhibit decreased histamine- and IgG-E-mediated leakage[56]. Inhibition of STAT3 phosphorylation decreases LPS-induced myocardial vascular permeability in a murine model[58]. A chemokine called eotaxin (i.e. CCL11) increases STAT3 phosphorylation and promotes vascular permeability in human coronary artery endothelial cells[57]. Taken together with the important role of STAT3 in modulating VEGF-mediated vascular permeability in vertebrate models presented here, studies collectively suggest STAT3 is a central regulator of vascular barrier integrity.

Considerable effort has been devoted to the development of STAT3 inhibitors as therapeutic agents. In addition to the important role of STAT3 in the pathogenesis of vascular disease, ischemia, and other tissue injuries, STAT3 is aberrantly overexpressed in many human tumor types and correlates with poor cancer

prognoses. Development of STAT3 peptide inhibitors stemmed from elucidating the crystal structure of the STAT3β homodimer and were designed to target the p-Y-peptide binding pocket within the STAT3 SH2 domain. However, the clinical applicability of these STAT3 peptide inhibitors has been hindered by their lack of stability and inability to cross membranes. Non-peptidic small molecule inhibitors of STAT3 exhibited promising in vivo activity in preclinical studies, but most of these STAT3 inhibitors failed to progress to clinical trials because they required medium-to-high micromolar concentrations to achieve sufficient activity and necessitated additional optimization in order to be systemically administered to human subjects. While developing and translating STAT3 inhibitors to the clinic has proven difficult because STAT3 is a transcription factor without intrinsic enzymatic activity[62], several compounds that inhibit either the function or expression of STAT3 are currently in clinical trials[63], including a double-stranded decoy oligonucleotide that competitively inhibits STAT3 interactions with its target gene promoter elements[64] and an antisense oligonucleotide inhibitor of STAT3 expression, AZD9150[65].

Pyrimethamine (PYR; Daraprim®) is a clinically available, FDA-approved agent that directly inhibits STAT3-dependent transcription. This anti-microbial drug was discovered as a new STAT3 inhibitor through a chemical library screen based on its ability to oppose the gene expression signature of STAT3[42,44]. PYR inhibits STAT3 phosphorylation and transcriptional activity at micromolar concentrations known to be routinely achieved in humans without toxicity[42]. In the current study, PYR suppresses STAT3 activation in endothelial cells as we observe decreased phosphorylation of STAT3 Y705 by immunofluorescence and immunoblotting. PYR treatment prevents VEGF-induced ZO-1 disorganization, which suggests that STAT3 inhibition improves tight junction instability in endothelium. We demonstrate that PYR administered to wildtype C57BL/6 mice substantially reduces VEGF-induced vascular permeability. Atovaquone (AQ; Mepron®), an FDA-approved anti-microbial agent with a strong human safety profile, has been shown to rapidly and specifically downregulate cell-surface expression of glycoprotein 130, which is required for STAT3 activation in multiple contexts[43]. Like PYR, we show that AQ stabilizes endothelial tight junctions in the presence of VEGF stimulation. Unlike PYR and AQ, C188-9 is a STAT3 inhibitor that targets the pY-peptide binding site within the STAT3 SH2 domain. C188-9 has been shown to inhibit G-CSF-induced STAT3 phosphorylation with low micromolar potency in AML cell lines[66] and subsequently has been well-established as an effective STAT3-specific inhibitor by various studies in models of cancer[46,67] and other diseases[68,69]. Here, we show that C188-9 inhibits VEGF-induced vascular permeability through in mouse models and cultured human endothelial cells. Our collective studies using three different STAT3 inhibitors suggest that suppression of STAT3 activity protects the endothelial barrier from VEGF-mediated vascular permeability. Future studies testing compounds that inhibit STAT3, particularly PYR and AQ given their clinical accessibility, in models of human diseases involving pathological vascular permeability are warranted.

**REFERENCES:**

1 Park-Windhol, C. & D'Amore, P. A. Disorders of Vascular Permeability. *Annual review of pathology* **11**, 251-281, doi:10.1146/annurev-pathol-012615-044506 (2016).

2 Senger, D. R. *et al.* Tumor cells secrete a vascular permeability factor that promotes accumulation of ascites fluid. *Science (New York, N.Y.)* **219**, 983-985, doi:10.1126/science.6823562 (1983).

3 Leung, D. W., Cachianes, G., Kuang, W. J., Goeddel, D. V. & Ferrara, N. Vascular endothelial growth factor is a secreted angiogenic mitogen. *Science (New York, N.Y.)* **246**, 1306-1309 (1989).

4 Carmeliet, P. *et al.* Abnormal blood vessel development and lethality in embryos lacking a single VEGF allele. *Nature* **380**, 435-439, doi:10.1038/380435a0 (1996).

5 Ferrara, N. *et al.* Heterozygous embryonic lethality induced by targeted inactivation of the VEGF gene. *Nature* **380**, 439-442, doi:10.1038/380439a0 (1996).

6 Nasevicius, A., Larson, J. & Ekker, S. C. Distinct requirements for zebrafish angiogenesis revealed by a VEGF-A morphant. *Yeast* **17**, 294-301, doi:10.1002/1097-0061(200012)17:4<294::AID-YEA54>3.0.CO;2-5 (2000).

7 Weis, S., Cui, J., Barnes, L. & Cheresh, D. Endothelial barrier disruption by VEGF-mediated Src activity potentiates tumor cell extravasation and metastasis. *The Journal of cell biology* **167**, 223-229, doi:10.1083/jcb.200408130 (2004).

8 Wu, Z. & McGoogan, J. M. Characteristics of and Important Lessons From the Coronavirus Disease 2019 (COVID-19) Outbreak in China: Summary of a Report of 72 314 Cases From the Chinese Center for Disease Control and Prevention. *Jama* **323**, 1239-1242, doi:10.1001/jama.2020.2648 (2020).

9 Teuwen, L. A., Geldhof, V., Pasut, A. & Carmeliet, P. COVID-19: the vasculature unleashed. *Nature reviews. Immunology* **20**, 389-391, doi:10.1038/s41577-020-0343-0 (2020).

10 Gallelli, L., Zhang, L., Wang, T. & Fu, F. Severe Acute Lung Injury Related to COVID-19 Infection: A Review and the Possible Role for Escin. *Journal of clinical pharmacology* **60**, 815-825, doi:10.1002/jcph.1644 (2020).

11 Xu, Z. *et al.* Pathological findings of COVID-19 associated with acute respiratory distress syndrome. *The Lancet. Respiratory medicine* **8**, 420-422, doi:10.1016/s2213-2600(20)30076-x (2020).

12 van Bruggen, N. *et al.* VEGF antagonism reduces edema formation and tissue damage after ischemia/reperfusion injury in the mouse brain. *J Clin Invest* **104**, 1613-1620, doi:10.1172/jci8218 (1999).

13 Navaratna, D., Guo, S., Arai, K. & Lo, E. H. Mechanisms and targets for angiogenic therapy after stroke. *Cell adhesion & migration* **3**, 216-223, doi:10.4161/cam.3.2.8396 (2009).

14 Huynh, J., Chand, A., Gough, D. & Ernst, M. Therapeutically exploiting STAT3 activity in cancer - using tissue repair as a road map. *Nat Rev Cancer* **19**, 82-96, doi:10.1038/s41568-018-0090-8 (2019).

15 Akira, S. *et al.* Molecular cloning of APRF, a novel IFN-stimulated gene factor 3 p91-related transcription factor involved in the gp130-mediated signaling pathway. *Cell* **77**, 63-71, doi:10.1016/0092-8674(94)90235-6 (1994).

16 Zhong, Z., Wen, Z. & Darnell, J. E., Jr. Stat3: a STAT family member activated by tyrosine phosphorylation in response to epidermal growth factor and interleukin-6. *Science (New York, N.Y.)* **264**, 95-98, doi:10.1126/science.8140422 (1994).

17 Kostromina, E. *et al.* Glucose intolerance and impaired insulin secretion in pancreas-specific signal transducer and activator of transcription-3 knockout mice are associated with microvascular alterations in the pancreas. *Endocrinology* **151**, 2050-2059, doi:10.1210/en.2009-1199 (2010).

18 Bartoli, M. *et al.* Vascular endothelial growth factor activates STAT proteins in aortic endothelial cells. *The Journal of biological chemistry* **275**, 33189-33192, doi:10.1074/jbc.C000318200 (2000).

19 Simons, M., Gordon, E. & Claesson-Welsh, L. Mechanisms and regulation of endothelial VEGF receptor signalling. *Nature reviews. Molecular cell biology* **17**, 611-625, doi:10.1038/nrm.2016.87 (2016).

20 Sasse, J. *et al.* Mutational analysis of acute-phase response factor/Stat3 activation and dimerization. *Molecular and cellular biology* **17**, 4677-4686, doi:10.1128/mcb.17.8.4677 (1997).

21 Rawlings, J. S., Rosler, K. M. & Harrison, D. A. The JAK/STAT signaling pathway. *Journal of cell science* **117**, 1281-1283, doi:10.1242/jcs.00963 (2004).

22 Bartoli, M. *et al.* VEGF differentially activates STAT3 in microvascular endothelial cells. *FASEB journal : official publication of the Federation of American Societies for Experimental Biology* **17**, 1562-1564, doi:10.1096/fj.02-1084fje (2003).

23 Chen, S. H. *et al.* Activated STAT3 is a mediator and biomarker of VEGF endothelial activation. *Cancer biology & therapy* **7**, 1994-2003 (2008).

24 Yahata, Y. *et al.* Nuclear translocation of phosphorylated STAT3 is essential for vascular endothelial growth factor-induced human dermal microvascular endothelial cell migration and tube formation. *The Journal of biological chemistry* **278**, 40026-40031, doi:10.1074/jbc.M301866200 (2003).

25 Yeh, H. H., Lai, W. W., Chen, H. H., Liu, H. S. & Su, W. C. Autocrine IL-6-induced Stat3 activation contributes to the pathogenesis of lung adenocarcinoma and malignant pleural effusion. *Oncogene* **25**, 4300-4309, doi:10.1038/sj.onc.1209464 (2006).

26 Zhao, D. *et al.* VEGF drives cancer-initiating stem cells through VEGFR-2/Stat3 signaling to upregulate Myc and Sox2. *Oncogene* **34**, 3107-3119, doi:10.1038/onc.2014.257 (2015).

27 Astone, M., Dankert, E. N., Alam, S. K. & Hoeppner, L. H. Fishing for cures: The alLURE of using zebrafish to develop precision oncology therapies. *NPJ Precis Oncol* **1**, doi:10.1038/s41698-017-0043-9 (2017).

28 Hoeppner, L. H. *et al.* Revealing the role of phospholipase Cbeta3 in the regulation of VEGF-induced vascular permeability. *Blood* **120**, 2167-2173, doi:10.1182/blood-2012-03-417824 (2012).

29 Hoeppner, L. H. *et al.* RhoC maintains vascular homeostasis by regulating VEGF-induced signaling in endothelial cells. *Journal of cell science* **128**, 3556-3568, doi:10.1242/jcs.167601 (2015).

30 Pei, W. *et al.* Guided genetic screen to identify genes essential in the regeneration of hair cells and other tissues. *NPJ Regen Med* **3**, 11, doi:10.1038/s41536-018-0050-7 (2018).

31 Petzold, A. M. *et al.* SCORE imaging: specimen in a corrected optical rotational enclosure. *Zebrafish* **7**, 149-154, doi:10.1089/zeb.2010.0660 (2010).

32 Dasgupta, M. *et al.* Critical role for lysine 685 in gene expression mediated by transcription factor unphosphorylated STAT3. *The Journal of biological chemistry* **289**, 30763-30771, doi:10.1074/jbc.M114.603894 (2014).
33 Tanaka, M., Gupta, R. & Mayer, B. J. Differential inhibition of signaling pathways by dominant-negative SH2/SH3 adapter proteins. *Molecular and cellular biology* **15**, 6829-6837, doi:10.1128/mcb.15.12.6829 (1995).
34 Horn, M. *et al.* DRE-1/FBXO11-dependent degradation of BLMP-1/BLIMP-1 governs C. elegans developmental timing and maturation. *Developmental cell* **28**, 697-710, doi:10.1016/j.devcel.2014.01.028 (2014).
35 Momand, J. *et al.* t-Darpp is an elongated monomer that binds calcium and is phosphorylated by cyclin-dependent kinases 1 and 5. *FEBS Open Bio* **7**, 1328-1337, doi:10.1002/2211-5463.12269 (2017).
36 Yu, Z. *et al.* Epithelium-Specific Ets-Like Transcription Factor 1, ESE-1, Regulates ICAM-1 Expression in Cultured Lung Epithelial Cell Lines. *Mediators of inflammation* **2015**, 547928, doi:10.1155/2015/547928 (2015).
37 Alam, S. K. *et al.* ASCL1-regulated DARPP-32 and t-DARPP stimulate small cell lung cancer growth and neuroendocrine tumour cell proliferation. *British journal of cancer* **123**, 819-832, doi:10.1038/s41416-020-0923-6 (2020).
38 Hillion, J. *et al.* The high-mobility group A1a/signal transducer and activator of transcription-3 axis: an achilles heel for hematopoietic malignancies? *Cancer research* **68**, 10121-10127, doi:10.1158/0008-5472.can-08-2121 (2008).
39 Takeda, K. *et al.* Targeted disruption of the mouse Stat3 gene leads to early embryonic lethality. *Proceedings of the National Academy of Sciences of the United States of America* **94**, 3801-3804, doi:10.1073/pnas.94.8.3801 (1997).
40 Kisanuki, Y. Y. *et al.* Tie2-Cre transgenic mice: a new model for endothelial cell-lineage analysis in vivo. *Developmental biology* **230**, 230-242, doi:10.1006/dbio.2000.0106 (2001).
41 Moh, A. *et al.* Role of STAT3 in liver regeneration: survival, DNA synthesis, inflammatory reaction and liver mass recovery. *Laboratory investigation; a journal of technical methods and pathology* **87**, 1018-1028, doi:10.1038/labinvest.3700630 (2007).
42 Khan, M. W. *et al.* The STAT3 inhibitor pyrimethamine displays anti-cancer and immune stimulatory effects in murine models of breast cancer. *Cancer immunology, immunotherapy : CII* **67**, 13-23, doi:10.1007/s00262-017-2057-0 (2018).
43 Xiang, M. *et al.* Gene expression-based discovery of atovaquone as a STAT3 inhibitor and anticancer agent. *Blood* **128**, 1845-1853, doi:10.1182/blood-2015-07-660506 (2016).
44 Takakura, A. *et al.* Pyrimethamine inhibits adult polycystic kidney disease by modulating STAT signaling pathways. *Hum Mol Genet* **20**, 4143-4154, doi:10.1093/hmg/ddr338 (2011).
45 Lampugnani, M. G. Endothelial cell-to-cell junctions: adhesion and signaling in physiology and pathology. *Cold Spring Harbor perspectives in medicine* **2**, doi:10.1101/cshperspect.a006528 (2012).
46 Bharadwaj, U. *et al.* Small-molecule inhibition of STAT3 in radioresistant head and neck squamous cell carcinoma. *Oncotarget* **7**, 26307-26330, doi:10.18632/oncotarget.8368 (2016).
47 Hoffmann, C. J. *et al.* Vascular signal transducer and activator of transcription-3 promotes angiogenesis and neuroplasticity long-term after stroke. *Circulation* **131**, 1772-1782, doi:10.1161/CIRCULATIONAHA.114.013003 (2015).
48 Wang, M. *et al.* Endothelial STAT3 plays a critical role in generalized myocardial proinflammatory and proapoptotic signaling. *Am J Physiol Heart Circ Physiol* **293**, H2101-2108, doi:10.1152/ajpheart.00125.2007 (2007).
49 Wei, D. *et al.* Stat3 activation regulates the expression of vascular endothelial growth factor and human pancreatic cancer angiogenesis and metastasis. *Oncogene* **22**, 319-329, doi:10.1038/sj.onc.1206122 (2003).
50 Huang, S. W., Lien, J. C., Kuo, S. C. & Huang, T. F. DDA suppresses angiogenesis and tumor growth of colorectal cancer in vivo through decreasing VEGFR2 signaling. *Oncotarget* **7**, 63124-63137, doi:10.18632/oncotarget.11152 (2016).
51 Niu, G. *et al.* Constitutive Stat3 activity up-regulates VEGF expression and tumor angiogenesis. *Oncogene* **21**, 2000-2008, doi:10.1038/sj.onc.1205260 (2002).
52 Park, J. S. *et al.* Interleukin-32beta stimulates migration of MDA-MB-231 and MCF-7cells via the VEGF-STAT3 signaling pathway. *Cell Oncol (Dordr)* **36**, 493-503, doi:10.1007/s13402-013-0154-4 (2013).

53 Kano, A. *et al.* Endothelial cells require STAT3 for protection against endotoxin-induced inflammation. *The Journal of experimental medicine* **198**, 1517-1525, doi:10.1084/jem.20030077 (2003).

54 Wang, M. *et al.* Sex differences in endothelial STAT3 mediate sex differences in myocardial inflammation. *Am J Physiol Endocrinol Metab* **293**, E872-877, doi:10.1152/ajpendo.00251.2007 (2007).

55 Alsaffar, H., Martino, N., Garrett, J. P. & Adam, A. P. Interleukin-6 promotes a sustained loss of endothelial barrier function via Janus kinase-mediated STAT3 phosphorylation and de novo protein synthesis. *Am J Physiol Cell Physiol* **314**, C589-C602, doi:10.1152/ajpcell.00235.2017 (2018).

56 Hox, V. *et al.* Diminution of signal transducer and activator of transcription 3 signaling inhibits vascular permeability and anaphylaxis. *The Journal of allergy and clinical immunology* **138**, 187-199, doi:10.1016/j.jaci.2015.11.024 (2016).

57 Jamaluddin, M. S. *et al.* Eotaxin increases monolayer permeability of human coronary artery endothelial cells. *Arteriosclerosis, thrombosis, and vascular biology* **29**, 2146-2152, doi:10.1161/ATVBAHA.109.194134 (2009).

58 Lee, J. E. *et al.* Janex-1, a JAK3 inhibitor, ameliorates tumor necrosis factor-alpha-induced expression of cell adhesion molecules and improves myocardial vascular permeability in endotoxemic mice. *Int J Mol Med* **29**, 864-870, doi:10.3892/ijmm.2012.920 (2012).

59 Tang, H. *et al.* An essential role for Stat3 in regulating IgG immune complex-induced pulmonary inflammation. *FASEB journal : official publication of the Federation of American Societies for Experimental Biology* **25**, 4292-4300, doi:10.1096/fj.11-187955 (2011).

60 Wei, L. H. *et al.* The role of IL-6 trans-signaling in vascular leakage: implications for ovarian hyperstimulation syndrome in a murine model. *J Clin Endocrinol Metab* **98**, E472-484, doi:10.1210/jc.2012-3462 (2013).

61 Yun, J. H. *et al.* Endothelial STAT3 Activation Increases Vascular Leakage Through Downregulating Tight Junction Proteins: Implications for Diabetic Retinopathy. *Journal of cellular physiology* **232**, 1123-1134, doi:10.1002/jcp.25575 (2017).

62 Wong, A. L. A. *et al.* Do STAT3 inhibitors have potential in the future for cancer therapy? *Expert opinion on investigational drugs* **26**, 883-887, doi:10.1080/13543784.2017.1351941 (2017).

63 Johnson, D. E., O'Keefe, R. A. & Grandis, J. R. Targeting the IL-6/JAK/STAT3 signalling axis in cancer. *Nature reviews. Clinical oncology* **15**, 234-248, doi:10.1038/nrclinonc.2018.8 (2018).

64 Sen, M. *et al.* First-in-human trial of a STAT3 decoy oligonucleotide in head and neck tumors: implications for cancer therapy. *Cancer discovery* **2**, 694-705, doi:10.1158/2159-8290.CD-12-0191 (2012).

65 Reilley, M. J. *et al.* STAT3 antisense oligonucleotide AZD9150 in a subset of patients with heavily pretreated lymphoma: results of a phase 1b trial. *Journal for immunotherapy of cancer* **6**, 119, doi:10.1186/s40425-018-0436-5 (2018).

66 Redell, M. S., Ruiz, M. J., Alonzo, T. A., Gerbing, R. B. & Tweardy, D. J. Stat3 signaling in acute myeloid leukemia: ligand-dependent and -independent activation and induction of apoptosis by a novel small-molecule Stat3 inhibitor. *Blood* **117**, 5701-5709, doi:10.1182/blood-2010-04-280123 (2011).

67 Lewis, K. M. *et al.* Small-molecule targeting of signal transducer and activator of transcription (STAT) 3 to treat non-small cell lung cancer. *Lung cancer (Amsterdam, Netherlands)* **90**, 182-190, doi:10.1016/j.lungcan.2015.09.014 (2015).

68 Gavino, A. C., Nahmod, K., Bharadwaj, U., Makedonas, G. & Tweardy, D. J. STAT3 inhibition prevents lung inflammation, remodeling, and accumulation of Th2 and Th17 cells in a murine asthma model. *Allergy* **71**, 1684-1692, doi:10.1111/all.12937 (2016).

69 Akinfenwa, P. Y., Bond, W. S., Ildefonso, C. J., Hurwitz, M. Y. & Hurwitz, R. L. Versican G1 domain enhances adenoviral-mediated transgene expression and can be modulated by inhibitors of the Janus kinase (JAK)/STAT and Src family kinase pathways. *The Journal of biological chemistry* **292**, 14381-14390, doi:10.1074/jbc.M116.773549 (2017).

**Acknowledgements:** This work was supported a Grant-in-Aid of Research, Artistry and Scholarship Program Award #380634 from the Office of Vice President of Research at the University of Minnesota, Institutional Research Grant #129819-IRG-16-189-58-IRG81 from the American Cancer Society, and The Hormel Foundation (to L.H.H.) as well as the Fifth District Eagles Cancer Telethon Postdoctoral Fellowship Award (to S.K.A.). We thank Dr. Anna C. Sundborger-Lunna, Dr. Veer Bhatt, Dr. George Aslanidi, and Dr. Karina Kortova at The Hormel Institute for technically supporting the purification the human STAT3 protein and sharing associated reagents. We are grateful to Christina E. Hernandez, Abbygail M. Coyle, and Erin N. Dankert for their contributions to this work as Summer Undergraduate Research Experience interns. We thank Dr. Jim Hu from the Hospital for Sick Children in Toronto, Ontario, Canada for generously sharing the pGL3-ICAM1 reporter vector. We thank The Hormel Institute and its staff for administrative, shared equipment, animal facility, and institutional support.

**Data availability:** Data pertaining to this study are included in the manuscript and Supplemental Figures. Additional datasets used and/or analyzed during the current study are available from the corresponding author upon request.

**Competing interests:** The authors declare no competing interests.

**Author contributions:** L.W. and M.A. performed vascular permeability studies in transgenic animals. L.W. completed vascular permeability studies in wildtype animals treated with pharmacological inhibitors. L.W. and M.A. conducted immunofluorescence and immunoprecipitation experiments. L.W., M.A., and Z.Z. completed immunoblotting studies. L.W. and S.K.A. performed in vitro kinase and luciferase transcriptional reporter assays. W.P. and S.M.B. generated and characterized STAT3 knockout zebrafish using CRISPR/Cas9 technology. D.A.F. provided technical and scientific support as well as shared compounds. L.W., M.A., S.K.A. and L.H.H. performed experimental troubleshooting, reviewed relevant scientific literature, and critically analyzed data. L.W. and L.H.H. prepared most figures and wrote the manuscript. L.H.H. conceived the original aims of this study, led the project, and acquired funding to complete the reported research. All authors approved the final version of this manuscript.

## SUPPLEMENTAL FIGURES:

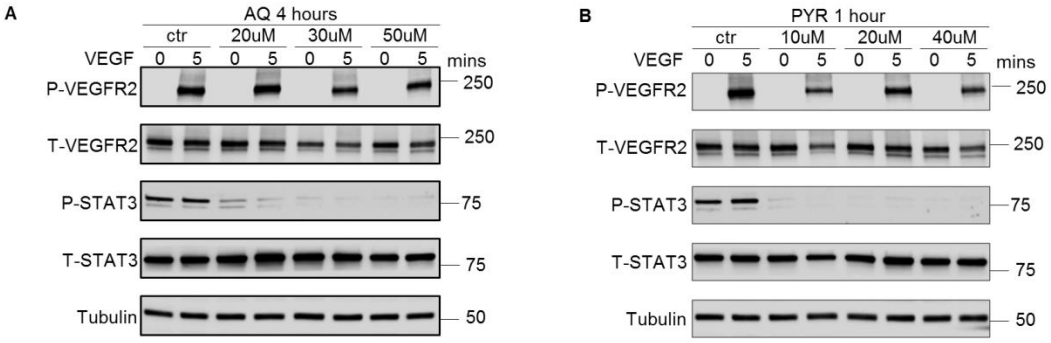


**Supplemental Figure 1: Optimization of STAT3 inhibitor dosing in VEGF-stimulated HUVEC.** Serum-starved HUVEC were pretreated with 0, 20, 30, or 50 µM AQ for 4 hours (left) or 0, 10, 20, or 40 µM PYR for 1 hour (right) prior to human VEGF-165 protein (25 ng/ml) stimulation for 0 or 5 minutes. Cells were lysed and then immunoblotted with primary antibodies.

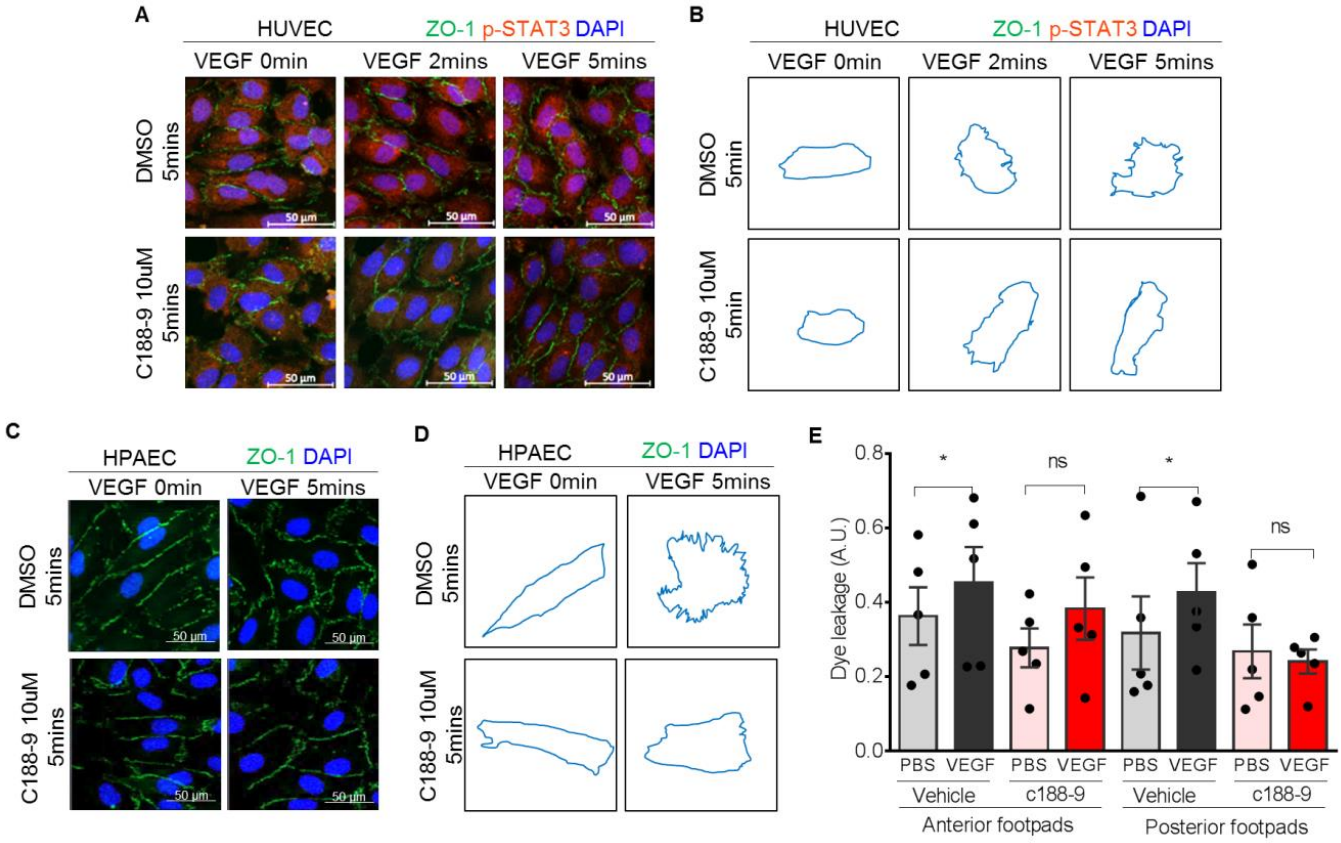


**Supplemental Figure 2: Pharmacological inhibition of STAT3 stabilizes endothelial barrier integrity following VEGF stimulation in HUVEC and mice.** (A) Serum-starved HUVECs were pretreated with 10uM C188-9 for 5 minutes prior to human VEGF-165 protein (25ng/ml) stimulation for 0, 2 and 5 minutes. VEGF stimulation promotes disorganization of ZO-1 (green) at endothelial cell junctions. ZO-1 organization is maintained when HUVEC were pretreated with C188-9. p-STAT3 (Y705; red) was reduced upon treatment with C188-9. Nuclei were stained with DAPI (blue). (B) Depiction of selected ZO-1 staining to help visualize its organization or disorganization upon VEGF treatment in the absence of STAT3 inhibitor, C188-9. (C) Serum-starved HPAEC were pretreated with 10uM C188-9 for 5 minutes prior to human VEGF-165 protein (25ng/ml) stimulation for 0 and 5 minutes. After stimulation with VEGF protein for 5 minutes, the structure of tight junction marked with ZO-1 was disrupted (i.e. jagged-like ZO-1 green staining). ZO-1 organization is maintained when HPAEC were pretreated with C188-9. Nuclei were stained with DAPI (blue). (D) Depiction of selected ZO-1 staining. (E) Mice were administered C188-9 or vehicle prior to tail vein injection with 1% Evans blue and VEGF (2.5 µg/ml) or PBS vehicle being injected into the root of the footpad. Quantitation of Evans blue leakage in C57BL/6 wildtype mice. n=5 mice per group. Each mouse was injected with PBS on right anterior and posterior footpads and VEGF on left anterior and posterior footpads. Multiple biological replicates were performed and depicted findings are representative. *P<0.05, paired t-test.